Hindawi Publishing Corporation
Journal of Nanomaterials
Volume 2012, Article ID 575926, 5 pages
doi:10.1155/2012/575926

*Research Article*

# Fabrication of Aligned Side-by-Side $TiO_2/SnO_2$ Nanofibers via Dual-Opposite-Spinneret Electrospinning

**Fu Xu,[1] Luming Li,[1] and Xiaojie Cui[2]**

[1] *School of Aerospace, Tsinghua University, Beijing 100084, China*
[2] *Department of Mechanical Engineering, Tsinghua University, Beijing 100084, China*

Correspondence should be addressed to Luming Li, lilm@mail.tsinghua.edu.cn

Received 18 October 2011; Revised 23 November 2011; Accepted 28 November 2011

Academic Editor: Tong Lin



Well-aligned and uniform side-by-side bicomponent fibers have been produced via dual-opposite-spinneret electrospinning. Side-by-side $TiO_2/SnO_2$ nanofibers were obtained after calcining as-spun fibers. The thermal degradation of the electrospun fibers was evaluated using combined thermogravimetry and differential thermal analysis (TG-DTA), and the crystal structure of calcined nanofibers was investigated by X-ray diffraction (XRD). The fabricated $TiO_2/SnO_2$ nanofibers expose both $TiO_2$ mainly consisting of anatase phase and rutile-type $SnO_2$ to the surface, which is appropriate for photocatalytic materials.

## 1. Introduction

Photocatalytic degradation of organic pollutants has been investigated widely in water and air purifications [1]. Hydrogen fuel production by photocatalytic water splitting [2] and high-efficiency solar cells [3] is thought to significantly mitigate the inadequacy of fossil fuels [4]. However, the narrow light-response range and the fast recombination of photogenerated charge carriers reduce the efficiency of photocatalytic reactions and therefore hinder the practicable applications of photocatalytic technique [5, 6].

Many studies have focused on new photocatalytic materials for fabricating high-efficiency photocatalysts. One strategy of fabricating new photocatalytic materials is forming a heterojunction between $TiO_2$ and other semiconductors, which could both extend the light-response range and reduce the recombination of photogenerated charge carriers [7]. Thin-film heterojunctions and particle heterojunctions have been fabricated via various methods: Kanai et al. [8] deposited $SnO_2/TiO_2$ ($TiO_2$ overcoated with $SnO_2$) thin-film stacks by reactive DC magnetron sputtering, and Tada et al. [9] produced patterned bilayer of $TiO_2/SnO_2$ ($SnO_2$ overcoated with $TiO_2$ stripes) using modified sol-gel method. One point to note is that these films were coated on substrates; thus, the photocatalyst lost approximately half of the contact surface between itself and reactants, which decreased the photocatalytic efficiency. On the other hand, coupled and capped semiconductor particles [10] may expose more surfaces to reactants, but it is difficult to separate powder photocatalysts from the solution after photocatalytic reaction. Therefore, nanofibers would be an appropriate structure for fabricating a type of photocatalyst with a large surface area exposed to reactants while maintaining good recoverability.

Electrospinning, regarded as a simple, low-cost, and universal technique for fabricating submicrofibers and nanofibers, has been receiving more and more attention over the last 15 years [11–13]. In addition to general beaded and nonbeaded thin nanofibers, other types of nanofibers with interesting morphology, such as core-shell nanofibers [14–16], hollow nanofibers [17], and side-by-side nanofibers [18, 19], have been produced by electrospinning. A side-by-side structure allows both parts of the nanofibers to be exposed to the surface. Bicomponent side-by-side $TiO_2/SnO_2$ nanofiber photocatalysts have been fabricated via side-by-side electrospinning [20]. Their study demonstrated that the photocatalytic degradation rate of Rhodamine B (RhB) dye on the side-by-side $TiO_2/SnO_2$ nanofibers was more than double that on the pure $TiO_2$ nanofibers.

In our previous work [21, 22], we have reported a dual-opposite-spinneret electrospinning (DOSE), which could

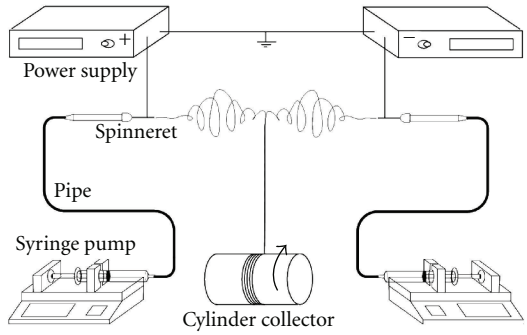


Scheme 1: Schematic diagram of dual-opposite-spinneret electrospinning apparatus.

effectively produce well-allied nanofibers. In this work, we report a new approach to fabricate side-by-side $TiO_2/SnO_2$ nanofibers using the DOSE.

## 2. Experimental Procedure

*2.1. Electrospinning Apparatus and Parameters.* The DOSE apparatus was illustrated in Scheme 1. Electrospinning solution was loaded into the syringe and pumped by the syringe pump. A flat-tipped stainless steel syringe needle was used as the spinneret. Two spinnerets were assembled horizontally in opposite directions, and each was connected to a separate high-voltage power supply. A rotating cylinder covered with aluminum foil was used as a collector.

The distance between the tips of two spinnerets was 12 cm, the applied voltages were +3100 V and −3100 V, the distance between the spinnerets and the collector was about 15 cm, the rotation rate of the cylinder collector (Diameter 10 cm) was $300\,\mathrm{r}\cdot\mathrm{min}^{-1}$. For fabricating $SnO_2/TiO_2$ bicomponent nanofibers, the feed rate of solution containing tetrabutyl titanate was $7.2\,\mu\mathrm{L}\cdot\mathrm{min}^{-1}$ and that of solution containing stannous octoate was $4.2\,\mu\mathrm{L}\cdot\mathrm{min}^{-1}$.

*2.2. Solutions and Calcining.* Solutions for electrospinning were prepared by dissolving polyvinylpyrrolidone (PVP, MW = 1 300 000) and tetrabutyl titanate or stannous octoate into a mixed solvent of ethanol and acetic acid (4 : 1, w/w). In a typical procedure, 2.5 g of tetrabutyl titanate was first dissolved into the mixed solvent, and then 2.4 g of PVP was added, following a constant magnetic stirring for 3 h at room temperature. In the two kinds of homogeneous electrospinning solution, both the concentrations of tetrabutyl titanate or stannous octoate were 11.1 wt%, while the concentration of PVP was 10.7 wt% and 11.5 wt%, respectively. Here, stannous octoate and tetrabutyl titanate were used as the precursors of $SnO_2$ and $TiO_2$, respectively. After electrospinning, the electrospun fibers were calcined at 500°C for 2 h in air environment, and side-by-side bicomponent $TiO_2/SnO_2$ nanofibers were fabricated.

*2.3. Characterization.* The electrospun fibers and calcined nanofibers were sputtered with gold, their morphologies were observed using field-emission scanning electron microscopy (FE-SEM, QUANTA 200 FEG) with an accelerating voltage of 15 kV, and the elemental mapping was conducted by energy-dispersive spectroscopy (EDS). The average diameter of fibers was measured from the SEM micrographs in original magnification of 2000x. Combined thermogravimetry and differential thermal analysis (TG-DTA) were carried out using simultaneous thermal analyzer (Netzsch STA 409) from 100 to 700°C at a heating rate of $10^\circ\mathrm{C}\cdot\mathrm{min}^{-1}$ in air atmosphere. The crystal structure of calcined fibers was investigated by X-ray diffraction (XRD, Rigaku D/Max-2500) using Cu K$\alpha$ radiation ($\lambda$ = 1.54056 Å).

## 3. Results and Discussion

In the DOSE process, two jets ejected from the opposite spinnerets and then merged into a single one, which was the great difference compared to the single spinneret electrospinning. This difference brought out two advantages. One advantage was that it was easy to get the well-aligned electrospun fibers. When the two oppositely charged jets merged into a single jet, the newly generated jet had an approximately neutral charge over all, which made it minimally affected by electric force. Therefore, it was easy to collect well-aligned and uniform electrospun fibers, as shown in Figure 1(a). The other advantage was that it was easy to make the side-by-side electrospun fibers. Before the two jets stuck together, some solvent had evaporated and jets had partially solidified, which prevented the mixing of the two parts of the newly generated jet. Thus, it was easy to make the side-by-side electrospun fibers, as shown in Figure 1(b) (partial enlarged views of this figure can be found in S1 Supplementary Material available online at doi: 10.1155/2012/575926). Specifically, it was meaningful when we wanted to make the side-by-side nanofibers from two miscible electrospun solutions. The obvious side-by-side structures were shown in Figures 2(a) and 2(b). There were distinct boundaries in the uniform side-by-side electrospun fibers and calcined nanofibers. Element components of the two parts were identified by EDS, as shown in Figure 2(c). One part contained element titanium (Ti) but no tin (Sn), while the other part contained both Ti and Sn. As Ti was easy to diffuse, the part coming from

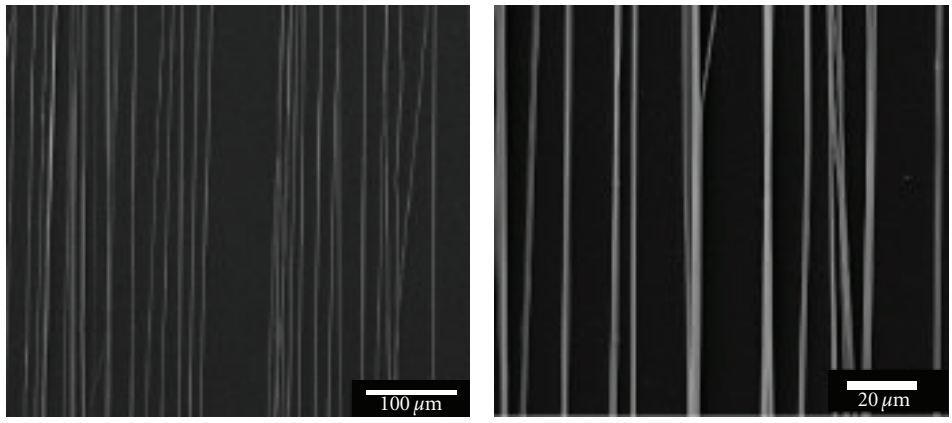


(a) (b)

Figure 1: Morphology of electrospun fibers by FE-SEM (a) well-aligned fibers, (b) side-by-side fibers.

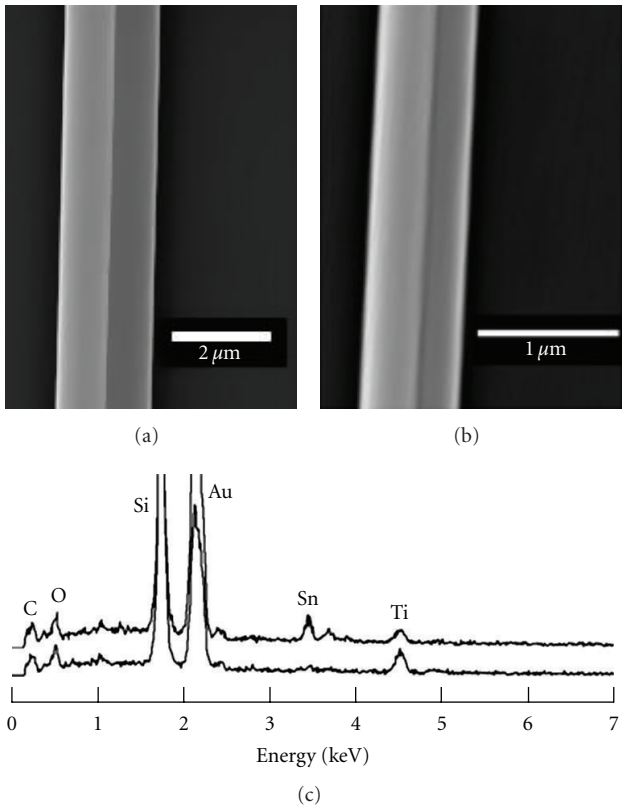


(a) (b) (c)

Figure 2: Detailed microstructure of side-by-side fiber by FE-SEM (a) electrospun fiber and (b) calcined nanofiber. (c) EDS spectrums of the fiber in (b).

electrospinning solution containing Sn also contained Ti after calcining.

The diameter of electrospun fibers in the experiment before calcining was $1.75 \pm 0.14\,\mu$m (average of 24 values). After calcining the diameter of nanofibers was much thinner, only $0.96 \pm 0.04\,\mu$m (average of 42 values). The main reason for the decrease in the diameter was the decomposition of PVP during the calcining process. During the calcining, process, the organic matter in electrospun fibers was decomposed, then amorphous $TiO_2(SnO_2)$ and crystalline $TiO_2(SnO_2)$ were formed sequentially. $TiO_2$ has three major different crystal structures: rutile, anatase and brookite, and crystal structures influence the property of photocatalyst. Therefore, it is necessary to investigate the thermal degradation of the electrospun fibers. Furthermore, considering the presence of the element Sn, $TiO_2/TiO_2$ side-by-side nanofibers were produced by DOSE using the same parameters except for a small change in feed rate of electrospinning solutions in order to stabilize the electrospinning process.

TG-DTA was carried out to evaluate the thermal degradation of the electrospun fibers. The simultaneous TG and DTA curves of the $TiO_2/SnO_2$ electrospun fibers and $TiO_2/TiO_2$ electrospun fibers were shown in Figure 3. Two groups of curves exhibited the same phenomenon in the temperature interval 180~360°C, which indicated that there was degradation of PVP on the side chain as well as decomposition of low-molecular-weight organic matter. In this step, electrospun fibers underwent approximately two-thirds of the total weight loss. The decomposition of the main chain of PVP and the amorphous-crystal phase transformation of metal oxides in fibers occurred around 400°C. The sharp peak in the DTA curve at 377°C in Figure 3(b) corresponded to the decomposition of the main chain of PVP, and the broad peak around 413°C corresponded to the crystallization of the $TiO_2$ anatase phase. There was only one peak around 400°C in DTA curve of Figure 3(a), a reasonable explanation was that the three peaks corresponding to decomposition of the main chain of PVP, crystallization of $TiO_2$, and crystallization of $SnO_2$, respectively, overlapped and composed this broad one. The unnoticeable peaks in both DTA curves centered at 550°C indicated the anatase-rutile phase transformation of $TiO_2$. The thermal degradation process was similar to the results of Nuansing et al. [23] and Park and Kim [24].

The XRD patterns of $TiO_2/SnO_2$ bicomponent nanofibers and $TiO_2/TiO_2$ nanofibers were shown in Figure 4. After calcination at 500°C for 2 h, almost pure anatase-type

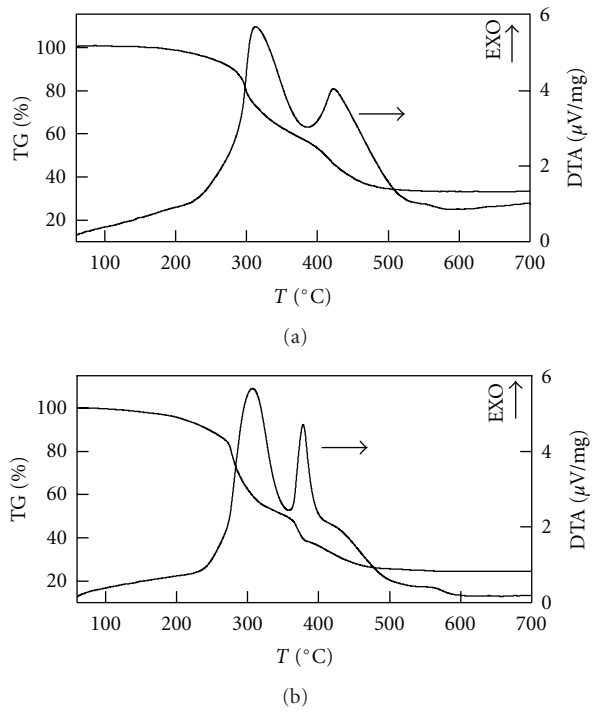


Figure 3: TG-DTA curves of thermal decomposition of the electrospun fibers: (a) $TiO_2/SnO_2$, (b) $TiO_2/TiO_2$, at a heating rate of $10^\circ C \cdot min^{-1}$ in air.

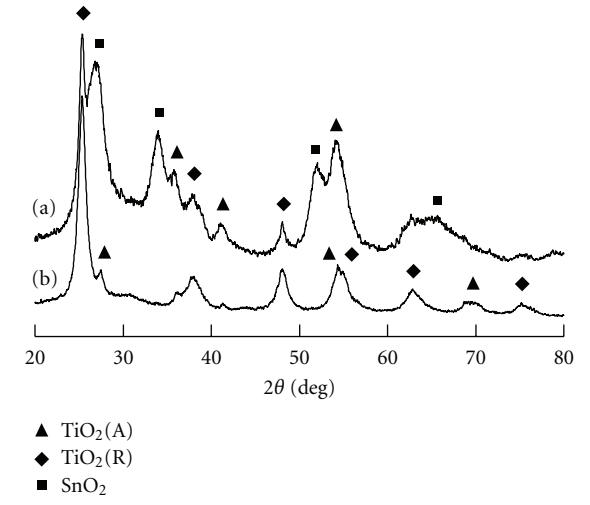


Figure 4: XRD patterns of calcined nanofibers: (a) $TiO_2/SnO_2$ (b) $TiO_2/TiO_2$, calcined at 500°C for 2 h.

$TiO_2$ was obtained except for a little rutile phase in the $TiO_2/TiO_2$ nanofiber, as shown in Figure 4(b). However, the calcined $TiO_2/SnO_2$ bicomponent nanofibers contained anatase-phase $TiO_2$, rutile-type $SnO_2$, and much more rutile-phase $TiO_2$ than $TiO_2/TiO_2$ nanofibers. The increase of rutile phase $TiO_2$ in bicomponent nanofibers was due to the presence of Sn. At a lower temperature, rutile-type $SnO_2$ had formed, which promoted the formation of rutile phase in $TiO_2$ [25].

The calcined side-by-side $TiO_2/SnO_2$ nanofiber possesses great potential in photocatalytic applications. Nanofibers with a side-by-side structure expose both $TiO_2$, mainly consisting of anatase phase and rutile-type $SnO_2$ to the surface. Because of the different band gaps of anatase $TiO_2$ and rutile $SnO_2$, the photogenerated electrons in these fibers would accumulate on one side, and photogenerated holes would accumulate on the other side. Therefore the recombination of photogenerated electrons and holes would greatly decrease, resulting in high photocatalytic activity.

## 4. Conclusion

Well-aligned and uniform side-by-side electrospun fibers were fabricated using the DOSE method. DOSE has great advantages for fabricating aligned side-by-side fibers: (a) because the jet instability is almost eliminated after the positive and negative charges neutralize each other, the electrospun bicomponent nanofibers produced via DOSE are well aligned and uniform; (b) because some solvent has evaporated and jets have partially solidified before the final jet is formed, there is much lower immiscibility requirement for making side-by-side structure between the two kinds of solutions used in electrospinning. $TiO_2/SnO_2$ side-by-side bicomponent nanofibers were obtained after being calcined in air at 500°C for 2 h. The fabricated $TiO_2/SnO_2$ nanofibers exposed both $TiO_2$ mainly consisting of anatase phase and rutile-type $SnO_2$ to the surface, which is appropriate for photocatalytic materials.

## Acknowledgment

This work was supported by the National Natural Science Foundation of China (Grant no. 60906050 and Grant no. 51077083).

## References

[1] M. R. Hoffmann, S. T. Martin, W. Choi, and D. W. Bahnemann, "Environmental applications of semiconductor photocatalysis," *Chemical Reviews*, vol. 95, no. 1, pp. 69–96, 1995.

[2] Z. Zou, J. Ye, K. Sayama, and H. Arakawa, "Direct splitting of water under visible light irradiation with an oxide semiconductor photocatalyst," *Nature*, vol. 414, no. 6864, pp. 625–627, 2001.

[3] T. Ma, M. Akiyama, E. Abe, and I. Imai, "High-efficiency dye-sensitized solar cell based on a nitrogen-doped nanostructured titania electrode," *Nano Letters*, vol. 5, no. 12, pp. 2543–2547, 2005.

[4] G. Liu, L. Wang, H. G. Yang, H. M. Cheng, and G. Q. Lu, "Titania-based photocatalysts—crystal growth, doping and heterostructuring," *Journal of Materials Chemistry*, vol. 20, no. 5, pp. 831–843, 2010.

[5] T. Ihara, M. Miyoshi, M. Ando, S. Sugihara, and Y. Iriyama, "Preparation of a visible-light-active $TiO_2$ photocatalyst by RF plasma treatment," *Journal of Materials Science*, vol. 36, no. 17, pp. 4201–4207, 2001.

[6] L. Zheng, Y. Zheng, C. Chen et al., "Network structured $SnO_2$/ZnO heterojunction nanocatalyst with high photocatalytic activity," *Inorganic Chemistry*, vol. 48, no. 5, pp. 1819–1825, 2009.

[7] S. Y. Chai, Y. J. Kim, M. H. Jung, A. K. Chakraborty, D. Jung, and W. I. Lee, "Heterojunctioned BiOCl/$Bi_2O_3$, a new visible light photocatalyst," *Journal of Catalysis*, vol. 262, no. 1, pp. 144–149, 2009.

[8] N. Kanai, T. Nuida, K. Ueta, K. Hashimoto, T. Watanabe, and H. Ohsaki, "Photocatalytic efficiency of $TiO_2$/$SnO_2$ thin film stacks prepared by DC magnetron sputtering," *Vacuum*, vol. 74, no. 3-4, pp. 723–727, 2004.

[9] H. Tada, A. Hattori, Y. Tokihisa, K. Imai, N. Tohge, and S. Ito, "A patterned-$TiO_2$/$SnO_2$ bilayer type photocatalyst," *Journal of Physical Chemistry B*, vol. 104, no. 19, pp. 4586–4587, 2000.

[10] I. Bedja and P. V. Kamat, "Capped semiconductor colloids. Synthesis and photoelectrochemical behavior of $TiO_2$-capped $SnO_2$ nanocrystallites," *Journal of Physical Chemistry*, vol. 99, no. 22, pp. 9182–9188, 1995.

[11] J. Doshi and D. H. Reneker, "Electrospinning process and applications of electrospun fibers," *Journal of Electrostatics*, vol. 35, no. 2-3, pp. 151–160, 1995.

[12] Z. M. Huang, Y. Z. Zhang, M. Kotaki, and S. Ramakrishna, "A review on polymer nanofibers by electrospinning and their applications in nanocomposites," *Composites Science and Technology*, vol. 63, no. 15, pp. 2223–2253, 2003.

[13] A. Greiner and J. H. Wendorff, "Electrospinning: a fascinating method for the preparation of ultrathin fibers," *Angewandte Chemie International Edition*, vol. 46, no. 30, pp. 5670–5703, 2007.

[14] Z. Sun, E. Zussman, A. L. Yarin, J. H. Wendorff, and A. Greiner, "Compound core-shell polymer nanofibers by co-electrospinning," *Advanced Materials*, vol. 15, no. 22, pp. 1929–1932, 2003.

[15] Y. Zhang, Z. M. Huang, X. Xu, C. T. Lim, and S. Ramakrishna, "Preparation of core-shell structured PCL-r-gelatin bi-component nanofibers by coaxial electrospinning," *Chemistry of Materials*, vol. 16, no. 18, pp. 3406–3409, 2004.

[16] A. V. Bazilevsky, A. L. Yarin, and C. M. Megaridis, "Co-electrospinning of core-shell fibers using a single-nozzle technique," *Langmuir*, vol. 23, no. 5, pp. 2311–2314, 2007.

[17] D. Li and Y. Xia, "Direct fabrication of composite and ceramic hollow nanofibers by electrospinning," *Nano Letters*, vol. 4, no. 5, pp. 933–938, 2004.

[18] P. Gupta and G. L. Wilkes, "Some investigations on the fiber formation by utilizing a side-by-side bicomponent electrospinning approach," *Polymer*, vol. 44, no. 20, pp. 6353–6359, 2003.

[19] T. Lin, H. Wang, and X. Wang, "Self-crimping bicomponent nanofibers electrospun from polyacrylonitrile and elastomeric polyurethane," *Advanced Materials*, vol. 17, no. 22, pp. 2699–2703, 2005.

[20] Z. Liu, D. D. Sun, P. Guo, and J. O. Leckie, "An efficient bicomponent $TiO_2$/$SnO_2$ nanofiber photocatalyst fabricated by electrospinning with a side-by-side dual spinneret method," *Nano Letters*, vol. 7, no. 4, pp. 1081–1085, 2007.

[21] H. Pan, L. Li, L. Hu, and X. Cui, "Continuous aligned polymer fibers produced by a modified electrospinning method," *Polymer*, vol. 47, no. 14, pp. 4901–4904, 2006.

[22] X. Cui, L. Li, J. Xu, and F. Xu, "Fabrication of continuous aligned polyvinylpyrrolidone fibers via electrospinning by elimination of the jet bending instability," *Journal of Applied Polymer Science*, vol. 116, no. 6, pp. 3676–3681, 2010.

[23] W. Nuansing, S. Ninmuang, W. Jarernboon, S. Maensiri, and S. Seraphin, "Structural characterization and morphology of electrospun $TiO_2$ nanofibers," *Materials Science and Engineering B*, vol. 131, no. 1–3, pp. 147–155, 2006.

[24] J. Y. Park and S. S. Kim, "Effects of processing parameters on the synthesis of $TiO_2$ nanofibers by electrospinning," *Metals and Materials International*, vol. 15, no. 1, pp. 95–99, 2009.

[25] R. Zhang, H. Wu, D. Lin, and W. Pan, "Preparation of necklace-structured $TiO_2$/$SnO_2$ hybrid nanofibers and their photocatalytic activity," *Journal of the American Ceramic Society*, vol. 92, no. 10, pp. 2463–2466, 2009.